Fabrication and Evaluation of ZnO Nanorods by Liquid-Phase Deposition

Takafumi Ichikawa* and Seimei Shiratori

*Department of Science and Technology, Keio University, 3-14-1 Hiyoshi Kohokuku,
Yokohamashi 223-8522, Japan*

The ZnO nanorod growth mechanism during liquid-phase deposition (LPD) has been investigated, with results considered in the context of phase stabilization, LPD chemical processes, and Gibbs free energy and entropy. Zinc oxide (ZnO) possesses unique optical and electronic properties, and obtaining ZnO species with high specific surface area is important in ZnO applications. Highly *c*-axis-oriented ZnO films are expected to be utilized in future optical and electrical devices. ZnO nanorods were synthesized using an aqueous solution deposition technique on a glass substrate with a free-standing ZnO nanoparticle layer. ZnO nanorod growth was easily controlled on the nanoscale by adjustment of the immersion time (15−210 min). X-ray diffraction, field-emission scanning electron microscopy (FE-SEM), and film thickness measurements were used to characterize the crystalline phase, orientation, morphology, microstructure, and growth mechanism of the ZnO nanorods. FE-SEM images were analyzed by image processing software, which revealed details of the of ZnO nanorod growth mechanism.

1. Introduction

There has been much recent attention focused on zinc oxide (ZnO) nanostructures because of their potentially useful properties, including their wide band gap (3.37 eV), large binding energy (60 meV), excellent chemical and thermal stability, transparency, biocompatibility, and wide electrical conductivity range.[1] ZnO has been extensively studied for use in nanoelectronic devices, including gas sensors,[2−5] varistors,[6] transistors,[7,8] light-emitting diodes,[9] photodiodes,[10] and solar cells.[11−15] ZnO probably has the largest family of nanostructures among materials exhibiting abundant nanostructure configurations. ZnO nanostructures highly oriented in the *c* axis possess attractive properties, including the ability to produce a photocurrent, and are expected to be incorporated into future optical and electrical devices. ZnO nanorods are highly *c*-axis-oriented nanostructures, which are easily synthesized by liquid-phase-deposition (LPD) techniques.[16]

LPD is a high-performance growth technique that is particularly attractive because of its low cost, low operating temperature, and environmental friendliness. LPD can be carried out on a large scale on any substrate, and such process attributes are necessary for application manufacturing, examples of which include optical device windows and low value-added products. A key issue for the technological application of ZnO nanorods is their controllable growth, and a fundamental understanding of their growth mechanism is essential.

In this study, highly *c*-axis-oriented ZnO nanorods were synthesized by LPD on a glass substrate with a free-standing ZnO nanoparticle layer. ZnO nanorod structure could be easily controlled by the immersion time (15−210 min). The ZnO nanorod growth mechanism was investigated by X-ray diffraction (XRD), field-emission scanning electron microscopy (FE-SEM), and film thickness measurements and image processing. Our results are considered in the context

*To whom correspondence should be addressed. E-mail: t.ichikawa729@gmail.com.

(1) Schmidt-Mende, L.; MacManus-Driscoll, J. L. *Mater. Today* **2007**, *10*, 40.
(2) Wan, Q.; Li, Q. H.; Chen, Y. J.; Wang, T. H.; He, X. L.; Li, J. P.; Lin, C. L. *Appl. Phys. Lett.* **2004**, *84*(18), 3654–3656.
(3) Rao, B. B. *Mater. Chem. Phys.* **2000**, *64*(1), 62–65.
(4) Seiyama, T.; Kata, A.; Fujiishi, K.; Nagatani, M. *Anal. Chem.* **1962**, *34*, 1502–1503.
(5) Wang, J. X.; Sun, X. W.; Yang, Y.; Huang, H.; Lee, Y. C.; Tan, O. K.; Vayssieres, L. *Nanotechnology* **2006**, *17*(19), 4995–4998.
(6) Sousa, V. C.; Segadaes, A. M.; Morelli, M. R.; Kiminami, R. *Int. J. Inorg. Mater.* **1999**, *1*(3), 235–241.
(7) Goldberger, J.; Sirbuly, D. J.; Law, M.; Yang, P. *J. Phys. Chem. B* **2005**, *109*(1), 9–14.
(8) Bae, H. S.; Yoon, M. H.; Kim, J. H.; Im, S. *Appl. Phys. Lett.* **2003**, *83*(25), 5313–5315.
(9) Saito, N.; Haneda, H.; Sekiguchi, T.; Ohashi, N.; Sakaguchi, I.; Koumoto, K. *Adv. Mater.* **2002**, *14*(6), 418–421.
(10) Sato, Y.; Kusumi, H.; Yamaguchi, H.; Komiyama, T.; Aoyama, T. *Physica B* **2006**, *376*, 719–721.
(11) Emrah Unalan, H.; Hiralal, P.; Kuo, D.; Parekh, B.; Amaratunga, G.; Chhowalla, M. *J. Mater. Chem* **2008**, DOI: 10.1039/b810748c.
(12) Greene, L. E.; Law, M.; Yuhas, B. D.; Yang, P. *J. Phys. Chem.* **2007**, *111*, 18451–18456.
(13) Olson, D. C.; Piris, J.; Collins, R. T.; Shaheen, S. E.; Ginley, D. S. *Thin Solid Films* **2006**, *496*, 26–29.
(14) Thitima, R.; Patcharee, C.; Takashi, S.; Susumu, Y. *Solid-State Electron.* **2009**, *53*, 176–180.
(15) Olson, D. C.; Lee, Y.-J.; White, M. S.; Kopidakis, N.; Shaheen, S. E.; Ginley, D. S.; Voigt, J. A.; Hsu, J. W. P. *J. Phys. Chem.* **2008**, *112*, 9544–9547.
(16) Yamabi, S.; Imai, H. *J. Am. Ceram. Soc.* **2002**, *92*(4), 3773–3778.

of phase stabilization, LPD chemical processes, and Gibbs free energy and entropy.

2. Experimental Method[17,18]

Slide glass (Matsunami microslide glass, Japan, 76 × 26 × 1 mm) was used as the supporting substrate and was ultrasonically cleaned with ultrapure water and aqueous KOH (Kanto Chemical Co., Inc., 86.0%). Experimental method details have been divided into two stages. The first was fabrication of the ZnO nanoparticle layer, and the second was fabrication of the ZnO nanorods.

i. Fabrication of the ZnO Nanoparticle Layer. A 40 mL solution of zinc acetate dehydrate [$Zn(CH_3COO)_2 \cdot 2H_2O$; Wako Pure Chemical Industries, Ltd., 99.0%], 2-methoxyethanol [$CH_3O(CH_2)_2OH$; Jusei Chemical Co., Ltd., 99.0%], and 2-aminoethanol ($NH_2CH_2CH_2OH$; Wako Pure Chemical Industries, Ltd., 99.0%) was stirred for 2 h at room temperature. The concentration of zinc acetate dehydrate was 0.5 M. A clean glass substrate was dip-coated by immersion in the solution and subsequently raised at 1 mm/s, which provided a zinc acetate dehydrate template layer. The coated slide was annealed at 200 °C for 1 h in air, which formed a free-standing ZnO nanoparticle layer on the glass.

ii. Fabrication of the ZnO Nanorods. A 100 mL solution of zinc nitrate hexahydrate [$Zn(NO_3)_26H_2O$; Wako Pure Chemical Industries, Ltd., 99.0%], ammonium chloride (NH_4Cl; Jusei Chemical Co., Ltd., 99.5%), urea [$CO(H_2N)_2$; Jusei Chemical Co., Ltd., 99.0%], and an ammonia solution (aqueous NH_3; Kanto Chemical Co., Inc., 28.0%) was stirred for 1 h at room temperature. The concentration of zinc nitrate hexahydrate was 0.1 M. The ZnO nanoparticle layered glass substrate was immersed in the solution at 90 °C for 15−210 min, which formed ZnO nanorods on the surface of the ZnO nanoparticle layer. Substrates were removed from solution, rinsed with ultrapure water, and then dried under N_2.

Fabrication of the ZnO nanorods has been reported using zinc acetate dihydrate at the second stage;[19] however, the solubility of zinc nitrate hexahydrate (127.8 g in 100 mL of water at 25 °C) is higher than that of zinc acetate dehydrate (40.0 g in 100 mL of water at 25 °C). Because of this, zinc nitrate hexahydrate was used instead at the second stage where water was the solvent.

The ZnO nanorod crystalline phase and orientation were examined using XRD (D8, DISCOVER, Bruker, Kanagawa, Japan) with Cu Kα radiation (40 kV, 40 mA), at a scan rate and a step size of 2°/min and 0.01°, respectively. The morphology and microstructure were observed using FE-SEM (S-4700, Hitachi, Tokyo, Japan), with an accelerating voltage of 5 kV. From frontal SEM images of ZnO nanorods, the average crystal width was calculated from the ratio with the internal scale. The ZnO film thicknesses for various immersion times were measured using film thickness measurements (Dektak; 3030, ULVAC, Tokyo, Japan). Frontal SEM images of ZnO nanorods were bicolored (white and black) using image treatment software (Adobe Photoshop CS4), where black and white represented free space and ZnO crystals, respectively. A black:white pixel ratio was measured to gauge the crystalline site occupancy. The crystal occupancy (Z) was calculated using the formula $Z (\%) = X/(X + Y) \times 100$, where X and Y are the number of white and black pixels, respectively. The surface temperatures of ZnO films immersed for various times were measured using an optics
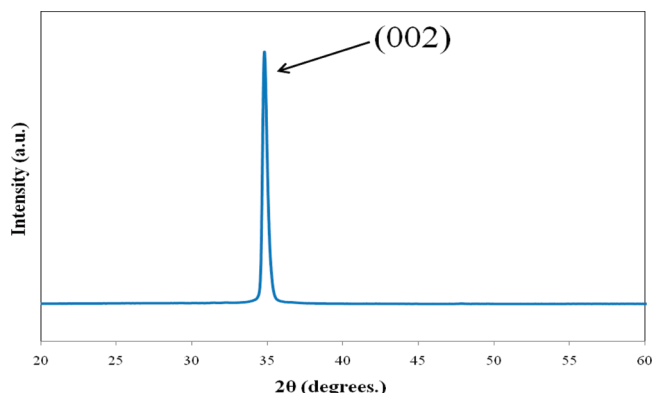
(17) Xiulan, H.; Yoshitake, M.; Tatsuki, O.; Kazumi, K. *J. Am. Ceram. Soc.* **2009**, *92*(4), 922−926.
(18) Sumio, S. *Agne* **1988**, 19−24.
(19) Qingwei, L.; Jiming, B.; Jingchang, S.; Jingwei, W.; Yingmin, L.; Kaitong, S.; Dongqi, Y. *Appl. Surf. Sci.* **2010**, *256*, 1698−1702.

Figure 1. XRD pattern of ZnO nanorods immersed for 90 min.

radiation thermometer (THERMO-HUNTER; PT-S80/U80, OPTEX, Siga, Japan).

3. Results and Discussion

Figure 1 shows the XRD pattern of ZnO nanorods immersed for 90 min, which was consistent with the standard JCPDS (no. 36-1451) pattern, indicating that the ZnO nanorods fabricated were of the wurtzite structure. An intense diffraction at 34° corresponding to the (002) plane indicated that ZnO crystals were preferentially oriented along the c axis (perpendicular to the substrate surface).

Figure 2 shows SEM images of the free-standing ZnO nanoparticle layer obtained from delamination during thermal treatment. The thermal decomposition of zinc acetate dehydrate occurred along with delamination, resulting in a free-standing ZnO layer, as shown in Figure 2a,b. These results suggested that thermal treatment of the zinc acetate dehydrate template layer played an essential role in forming the free-standing ZnO nanoparticle layer, because of the difference in thermal expansion between the glass and ZnO nanoparticles.[20] The ZnO nanoparticles had a diameter of ∼40 nm. During aqueous solution deposition, ZnO nanorods self-selectively grew on the entire ZnO nanoparticle surface by heterogeneous nucleation and growth because of the lower nucleation free energy.

Figures 3 and 4 show front and cross-sectional SEM images of ZnO nanorods, respectively, as a function of the growth time from 15 to 210 min. ZnO nanorods with a wurtzite structure were vertical, well-aligned, and uniformly distributed on the glass substrate. The ZnO nanorod crystal length increased up to 90 min of immersion time and then stopped growing with further immersion (Figure 3). ZnO nanorods widely spaced (30, 60, and 90 min) and narrowly spaced (15, 45, and 75 min) were apparent at alternating immersion times prior to 90 min. From these results, it was clear that ZnO nanorods grew only prior to 90 min of immersion time. ZnO nanorod growth could be predicted prior to 90 min of immersion time. The ZnO nanorod length (or film thickness, as depicted in Figure 5) increased prior to 90 min of immersion time and then stopped (Figure 4). As with frontal SEM images, cross-sectional images also showed growth up to 90 min of immersion time. Figure 5 shows a schematic view of ZnO nanorods, in which the crystal width and thickness are illustrated for clarity.

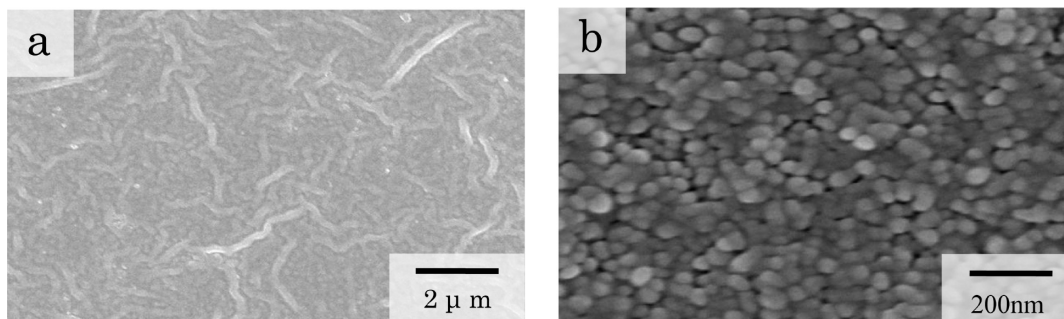(20) National Astronomical Observatory of Japan. *Chronological Scientific Tables*; MARUZEN: Tokyo, 2008.

Figure 2. SEM images of the free-standing ZnO nanoparticle layer: (a) 10K×; (b) 100K×.
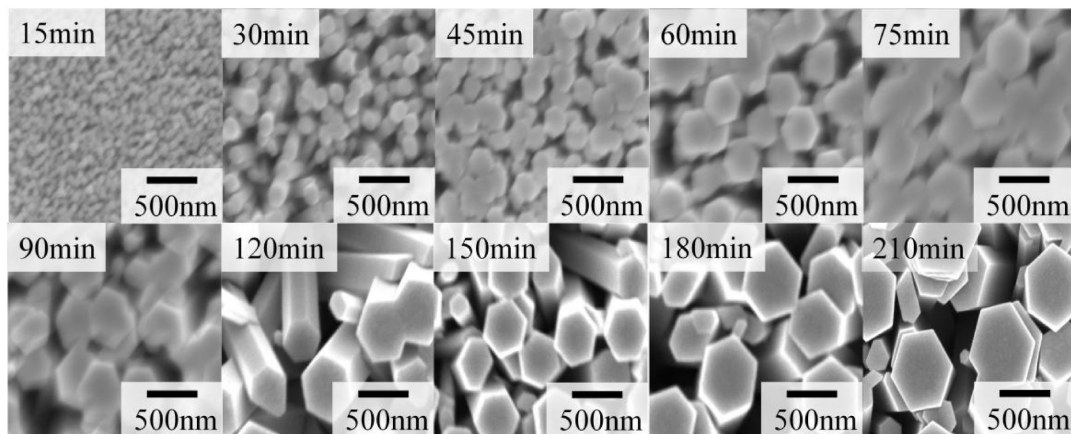

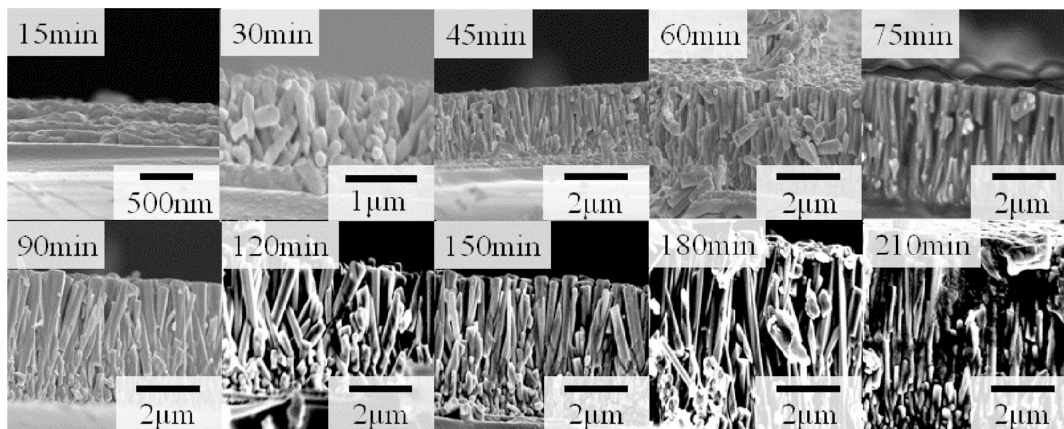**Figure 3.** Frontal SEM images of ZnO nanorods at 50K× magnification.

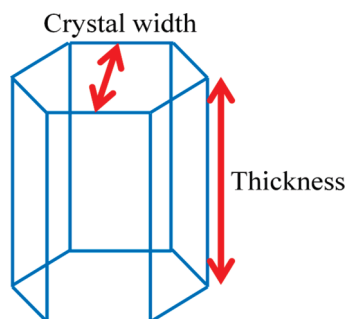**Figure 4.** Cross-sectional SEM images of ZnO nanorods.

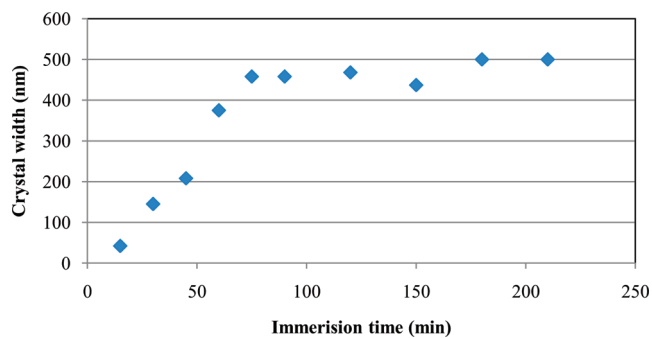**Figure 5.** Schematic view of ZnO nanorods.

Figure 6. Relationship between the crystal width and immersion time.
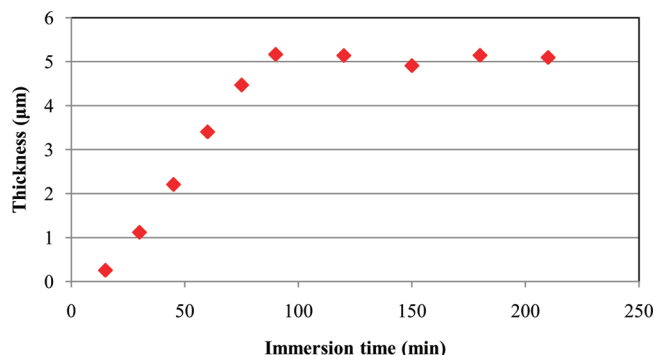
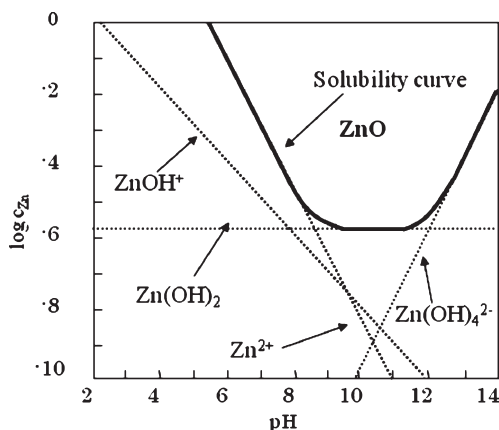**Figure 7.** Relationship between the film thickness and immersion time.

Figure 8. Phase stability diagram for aqueous ZnO species as a function of the pH.

Figure 6 shows the relationship between the average crystal width and immersion time, from which the average crystal width increased linearly up to 90 min of immersion time and then stopped. The average crystal width eventually became constant at ~500 nm.

Figure 7 shows the relationship between the ZnO film thickness and immersion time, from which the thickness increased linearly up to 90 min of immersion time and then stopped. The ZnO film thickness eventually became constant at ~5 μm.

A mechanism for the effect of the immersion time was obtained by considering phase stabilization, the chemical processes occurring during LPD, and the Gibbs free energy of the respective species.

Phase stabilization was considered first.[19] Figure 8 shows the phase stabilization diagram of aqueous ZnO species as a function of the pH. Dotted lines show the thermodynamic equilibrium between solid and solution species, calculated from thermodynamic data. Solid lines show the solubility of solid phases. ZnO is formed within the area enclosed by the solubility curve. Hydroxy complexes like $Zn(OH)_2$ and $Zn(NH_3)_4^{2+}$ are predominant in strongly alkaline conditions, and it is thought that dehydration reactions take place under such conditions. We suggest that hydroxyl groups at the crystal interface caused this dehydration reaction and that ZnO binding then occurred. ZnO nanorods with a wurtzite structure were finally formed. Zinc nitrate hexahydrate
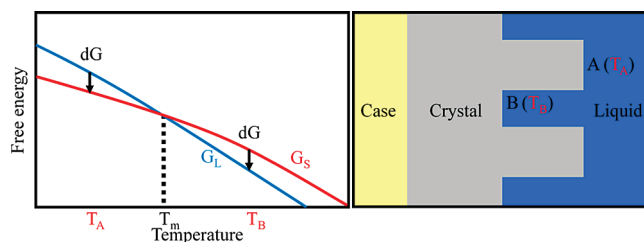
(21) Xu, S.; Lao, C.; Weintraub, B.; Wang, Z. L. *J. Mater. Res.* **2008**, *23*, 2072.

Figure 9. Relationship between the free energy and solution temperature. T_A is the ZnO nanorod surface temperature, T_B is the temperature at the base of the ZnO nanorods, T_m is the phase transition temperature, and G_L and G_S is the change in the free energy of the liquid and solid, respectively.
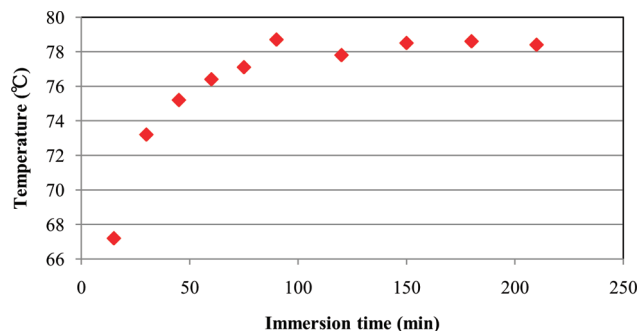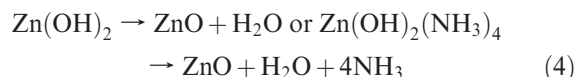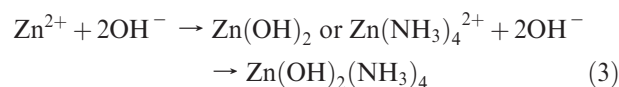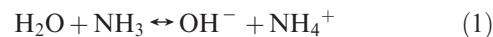

Figure 10. Relationship between the ZnO film surface temperature and immersion time.

provided Zn^{2+} ions required for the building of ZnO nanorods, and water molecules provided O^{2-} ions.[21] Detailed chemical reactions are as follows:

$$H_2O + NH_3 \leftrightarrow OH^- + NH_4^+ \tag{1}$$

$$Zn^{2+} + 4NH_3 \leftrightarrow Zn(NH_3)_4^{2+} \tag{2}$$

$$Zn^{2+} + 2OH^- \rightarrow Zn(OH)_2 \text{ or } Zn(NH_3)_4^{2+} + 2OH^- \rightarrow Zn(OH)_2(NH_3)_4 \tag{3}$$

$$Zn(OH)_2 \rightarrow ZnO + H_2O \text{ or } Zn(OH)_2(NH_3)_4 \rightarrow ZnO + H_2O + 4NH_3 \tag{4}$$

The Gibbs free energy was considered next.[22] If the formula for the Gibbs free energy (eq 5) is completely total and partially differentiated, eqs 6 and 7 are obtained, respectively, where G is the free energy, U is the internal energy, P is the pressure, V is the volume, T is the temperature, and S is the entropy.

$$G = U + PV - TS \tag{5}$$

$$dG = V\,dp - S\,dT \tag{6}$$

$$(\partial G/\partial T)_p = -SS > 0 \tag{7}$$

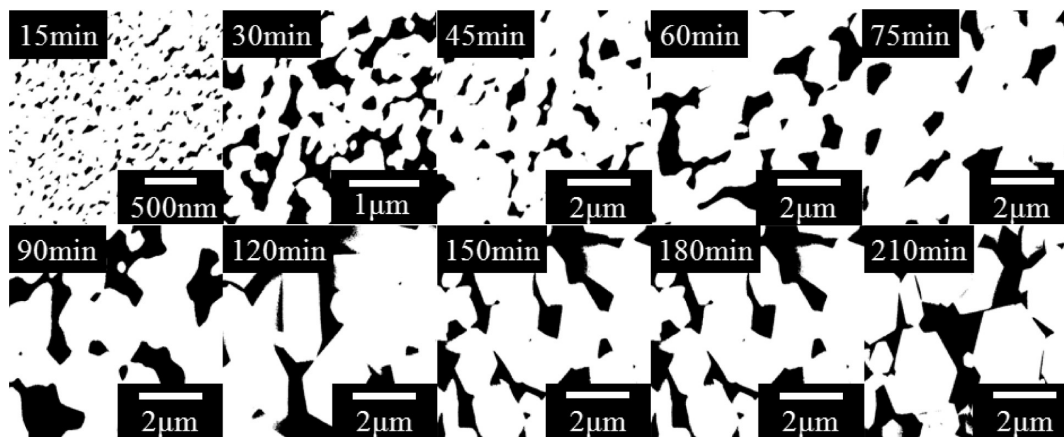(22) Ohno, K. *Thermodynamics studied from base*; Iwanami: Tokyo, 2001.

Figure 11. SEM images of ZnO nanorods after computational image treatment, at immersion times as stated.
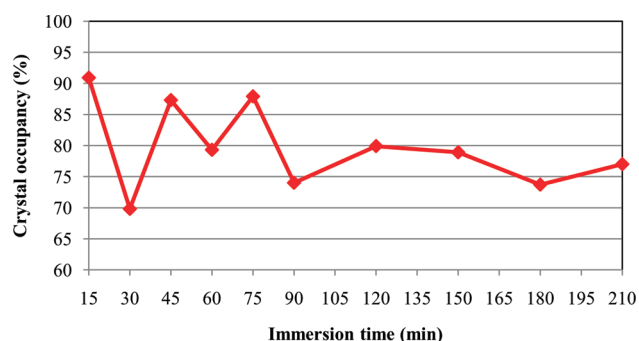

Figure 12. Relationship between the crystal occupancy and immersion time.

Figure 9 illustrates this concept, where the absolute temperature is shown by the horizontal axis and the free energy by vertical axis. The gradient shows a constant decrease. ZnO nanorod growth is thought to be endothermic, so the ZnO nanorod surface temperature (T_A) is lower than the temperature at the base of the ZnO nanorods (T_B). G_L and G_S represent the change in the free energy of the liquid and solid, respectively. According to the theory that the state variation of the material advances toward the direction where the free energy is the lowest, the ZnO nanorod surface would continue to change from liquid to solid until T_A reached the phase transition temperature (T_m). The base of the ZnO nanorods would continue to change from solid to liquid until T_B drops to T_m, and finally ZnO nanorods would be formed. When the surface temperature (T_A) and T_B both reached the same T_m, the change in the free energy was lost and nanorod growth stopped.

Figure 10 shows the relationship between the temperature and immersion time, where T_A increased linearly up to 90 min of immersion time and then stopped, confirming the validity of our Gibbs free energy model.

ZnO nanorod growth has been previously shown to correspond to the law of increasing entropy.[23] Because entropy is a function of state, the change in entropy accompanying a change of state must always be the same however the change of state occurs. The following formula describes entropic changes, for any infinitesimal change where the

equality must apply for a reversible change:

$$dS \geq \frac{dQ}{T} \tag{8}$$

where T is the temperature at which heat is applied to the system. Equation 8 is important because it contains all information regarding the efficiency and irreversibility in thermal processes.

For a thermally isolated system, $dQ = 0$, and applying eq 8 gives $dS \geq 0$. This is known as the law of increase of entropy, which states that the entropy of an isolated system cannot decrease. In the current study, ZnO nanorod growth can be considered as an isolated system because the temperature was controlled by the heating device (90 °C). Consider two bodies, 1 and 2, which are at temperatures T_1 and T_2, respectively. When the thermal capacity of the state C is assumed to be constant, the state can semistatically absorb the external heat quantity $dQ = C\,dT$. The total change in entropy is

$$\Delta S = \int \frac{dQ}{T} = \int_{T_1}^{T_2} \frac{C\,dT}{T} = C \log \frac{T_2}{T_1} \tag{9}$$

The ZnO nanorod surface temperature constantly increased up to 90 min of immersion time (Figure 10). In this range, $T_1 < T_2$, so

$$\Delta S > 0 \tag{10}$$

The ZnO nanorod surface temperature remained nearly constant after 90 min of immersion time (Figure 10). In this range, $T_1 = T_2$, so

$$\Delta S = 0 \tag{11}$$

From eqs 10 and 11, the total change of entropy becomes

$$\Delta S \geq 0 \tag{12}$$

ZnO nanorod growth was irreversible up to 90 min of immersion time and reversible at subsequent immersion times. Thus, ZnO nanorod growth corresponded to the law of increase of entropy.

Figure 11 shows SEM images of ZnO nanorods after image treatment, and Figure 12 shows the relationship between the ZnO nanorod crystal occupancy and immersion time. The crystal occupancy appeared to alternate up to 90 min of

(23) Adkins, C. J. *Equilibrium Thermodynamics*; Cambridge University Press: Cambridge, U.K., 1968.
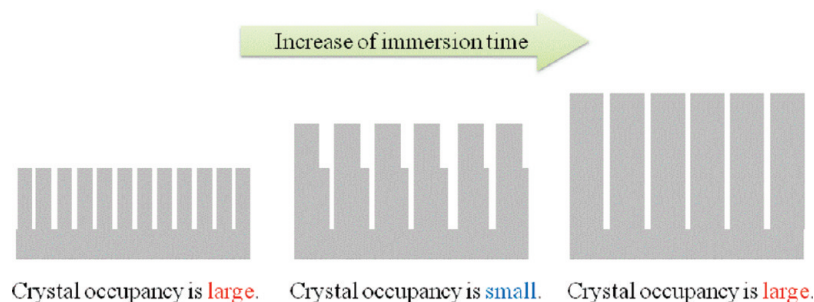
Figure 13. Schematic of the ZnO nanorod growth process prior to 90 min of immersion time.

immersion time and became constant with subsequent time. ZnO nanorod growth could be depicted diagrammatically, as shown in Figure 13. A portion of the nanorod grew in the c-axis direction, and the crystal occupancy subsequently decreased. Nanorods then grew in all directions, and the crystal occupancy subsequently increased. We suggest that only some nanorods reached equilibrium with a stable free energy, so some ZnO nanorods stopped growing while others continued to do so.

4. Conclusions

ZnO nanorods were fabricated using low-temperature LPD from a free-standing ZnO nanoparticle layer. Thermal treatment of the zinc acetate dehydrate layer resulted in the formation and delamination of the ZnO nanoparticle layer. ZnO nanorods grew on the entire surface of the free-standing ZnO nanoparticles layer by heterogeneous nucleation and growth, preferentially oriented along the c axis. ZnO nanorod growth could be easily controlled by the immersion time. A growth mechanism was proposed based on phase stabilization, LPD chemical processes, and Gibbs free energy and entropy. The high-optical-quality ZnO nanorods prepared have potential in applications including UV lasers, light-emitting diodes, and vertical field-effect transistor arrays.